The Use of Cluster Analysis to Classify Wear Particle Shapes

Mohammad S. Laghari [1,*], Ahmed Hassan [2], Addy Wahyudie [1], Mahmoud Haggag [2], and Abdulrahman Alraeesi [3]

[1] Department of Electrical and Communication Engineering, College of Engineering, United Arab Emirates University, Al Ain, United Arab Emirates
[2] Department of Architectural Engineering, College of Engineering, United Arab Emirates University, Al Ain, United Arab Emirates
[3] Department of Chemical Engineering, College of Engineering, United Arab Emirates University, Al Ain, United Arab Emirates
Email: mslaghari@uaeu.ac.ae (M.S.L.); ahmed.hassan@uaeu.ac.ae (A.H.); addy.w@uaeu.ac.ae (A.W.); mhaggag@uaeu.ac.ae (M.H.); a.araeesi@uaeu.ac.ae (A.A.)
*Corresponding author

***Abstract*—Microscopic wear particles carried by lubricating oil provide important diagnostic information about machine condition, wear mechanisms, and potential failure modes. Conventional wear-particle analysis frequently relies on professional visual interpretation, which may be subjective, labor-intensive, and challenging to replicate. This study presents an automated framework for classifying wear-particle shapes by integrating image processing, Fourier descriptor-based feature extraction, and hierarchical cluster analysis. Six common wear-particle types are considered: rubbing, severe sliding, cutting, fatigue, chunky, and spherical particles. Particle boundaries are extracted from microscopic images and represented using three Fourier descriptor formulations: Radial, Theta, and XY descriptors. These descriptors transform particle profiles into invariant coefficient features that are robust to changes in size, position, and orientation. The resulting feature vectors are evaluated using hierarchical clustering with Euclidean distance and average linkage. Comparative analysis indicates that the XY Fourier descriptor provides the most effective shape representation, producing more compact and better-separated clusters than the Radial and Theta descriptors. It then groups particles with similar morphological traits, supporting accurate and objective classification. Quantitative validation using the Silhouette Score and Davies–Bouldin Index further confirms the superior clustering performance of the XY descriptor. The proposed framework provides an objective and computationally efficient approach for wear-particle classification and supports condition-based maintenance by reducing reliance on manual expert assessment.**

***Keywords*—wear particle analysis, Fourier descriptors, cluster analysis, image processing, morphological classification**

I. Introduction

Computer vision-based wear particle analysis utilizes machine learning, Fourier-based form descriptors, and image processing to automatically classify microscopic wear particles. This reduces the need for human expertise and enables the early detection of equipment failure mechanisms.

Ferrography captures particle images. These images are then preprocessed using edge detection, segmentation, and noise reduction techniques. Profiles are then analyzed using local features, such as curvature and corner segments, and global features, such as area, perimeter, and Fourier coefficients. Radial, Theta, and XY Fourier descriptors are used to produce feature representations that are invariant to scale, translation, and rotation.

An interactive platform coordinates these processes to forecast wear failure modes and extract quantitative measures that feed into classifiers. These classifiers can range from neural networks and support vector machines to deep learning architectures such as ResNet50 and Vision Transformers. Deployments of engine, turbine, and hydraulic systems have demonstrated increased precision, throughput, and notable cost reductions. Nevertheless, issues persist with overlapping particles, low-contrast images, and the standardization of imaging procedures.

Wear particles are captured, resulting in images with varying levels of contrast and noise. Standard preprocessing methods include grayscale conversion, adaptive thresholding, edge-based segmentation to separate individual particles, and Gaussian or median filtering for noise reduction. Particle masks are refined through morphological processes such as dilation and erosion, and curvature analysis can enhance edge detection for precise boundary delineation.

Global descriptors that quantify general form qualities include area, perimeter, compactness, and the coefficients of Fourier series expansions. Fourier descriptors compactly capture shape complexity by converting each particle's closed contour into frequency-domain coefficients. These coefficients act as coordinates in a

Manuscript received January 27, 2026; revised March 3, 2026; accepted May 9, 2026; published August 26, 2026.

multidimensional feature space that may be clustered and classified.

Line segments, corner curvature, and edge roughness are the boundary characteristics that are the focus of local analysis. Curvature scale-space and fractal dimension are two methods that quantify tiny features along the contour and help separate smoother polymeric particles from sharp-edged metallic particles.

The three Fourier descriptors are examined in greater detail. Theta descriptors show the angular fluctuation of the contour radius, whereas radial Fourier descriptors encode the distance between the centroid and contour points as a periodic function. Robust particle comparisons are made possible by satisfying invariance to translation, rotation, scaling, and the choice of starting point. Higher-order descriptors capture finer details and irregularities, whereas lower-order descriptors capture general shape characteristics (elongation, triangularity, etc.).

The XY Fourier descriptor is a mathematical representation used to characterize the shape of a Two-Dimensional (2D) object from its boundary coordinates in the Cartesian plane. This method first converts the object's contour into a set of complex numbers.

Six wear-particle types are considered in this investigation: rubbing, severe sliding, cutting, fatigue, chunky, and spherical.

It is important to note that the present study focuses on the design and evaluation of Fourier descriptor-based shape representations within an unsupervised clustering framework, rather than on training a specific supervised classifier. In particular, we compare Radial, Theta, and XY Fourier descriptors using standard indices of clustering validity. The resulting XY descriptor is, however, readily usable as an input feature space for supervised classifiers such as Support Vector Machines (SVMs) or Convolutional Neural Networks (CNNs) in future work.

II. LITERATURE REVIEW

Earlier automated wear-particle studies used neural-network-based classification, while more recent approaches integrate deep convolutional networks and Vision Transformer architectures such as ResNet50/SepViT to address complex backgrounds, overlapping particles, and small targets [1, 2]. Support vector machines have also shown promise for morphological classification when combined with capacitive sensing data and smaller datasets [3].

Yuan *et al.* [4] proposed a radial-concave deviation-based method to extract features related to the size and shape of wear particles. They evaluated several classifiers for particle classification, including regression trees, naive Bayes, linear and quadratic discriminant analysis, and general classification methods. Their findings reported Classification and Regression Trees (CART) as the best-performing classifier among the tested models using features derived from the radial concave deviation approach.

The study presents several methods for locating and examining wear particles. Peng and Wang [5] employed a deep neural network to distinguish fatigue, oxide, and spherical wear particles, thereby overcoming the challenges posed by overlapping particles. They used a transfer learning approach based on the Inception-v3 model for feature extraction and classification. They explicitly added a fully connected layer after the classification layer to match the last layers of Inception-v3, thereby enhancing the model's ability to distinguish among various particle types.

Li *et al.* [6] applied an Extreme Learning Machine (ELM) approach to the recognition of Ferrographic wear particles. Their results demonstrated the usefulness of machine learning models for automated particle classification based on image features.

Stachowiak *et al.* [7] developed an automated method for classifying fatigue, abrasive, and adhesive wear particles based on surface texture and shape features. Their study used Scanning Electron Microscopy (SEM) images to build a wear-particle database and extracted texture information using a combination of Discrete Wavelet Transform (DWT) and statistical co-occurrence features.

Wu *et al.* [8] proposed an online fluid-monitoring system to evaluate wear particles. They used thresholding and background subtraction techniques to segment the Region of Interest (ROI). Following segmentation, the particles were analyzed using multi-view images to extract features such as spatial diameter, sphericity, height-to-aspect ratio, and other morphological characteristics.

You *et al.* [9] examined the application of a Multi-level Feature-Reused U-Net (MRF U-Net) for the precise segmentation of minute wear particles in oil-abrasive images. The suggested method augments the residual link strategy of U-Net to enhance the detection of minute wear particles in Ferrograms, thereby improving segmentation performance.

This study introduced TCBGY-Net—Transformer Convolutional Block Attention Mechanism Ghost BiFPN-YOLOv5 Network—to address several problems, including false detections, missed detections of small wear particles, difficulty distinguishing overlapping particles, and complex backgrounds in Ferrographic images. The proposed TCBGY-Net uses YOLOv5s as its backbone and enhances it with several advanced modules to improve detection performance [10].

This study proposes an intelligent method for recognizing images of Ferrography wear particles using an improved Mask R-CNN model. By enhancing feature extraction and integrating attention mechanisms, the model accurately detects, segments, and classifies wear particles while measuring their number and coverage area. The results show high accuracy and efficiency, making the approach useful for assessing wear severity and supporting maintenance decisions [11].

This research employs Fourier series, image processing techniques, and Fourier descriptors to analyze microscopic particles generated by wear mechanisms. An interactive image analysis system processes and stores quantitative information extracted from the particle profile. To identify particle profile features and facilitate systematic analysis of the profiles, an additional analysis of the stored data is presented. This analysis is displayed as three Fourier descriptors [12].

Laghari [13] investigated wear-particle profile analysis using Fourier analysis, highlighting the usefulness of frequency-domain shape representation for particle characterization. Quantitative information from the particle profile is processed and stored using an interactive image analysis system. The data is further analyzed using two Fourier descriptors. These descriptors enable systematic profile analysis and feature extraction from wear-particle profiles.

This study uses used-oil Ferrographic analysis as a maintenance method to check for wear in machine parts made of AISI 1045 medium-carbon steel. Wear particles were analyzed using a Direct Reading (DR) Ferrograph, a Ferrogram maker, and an optical microscope to measure particle characteristics and identify wear modes, including oxidation, corrosion, adhesion, and abrasion. The findings help evaluate wear severity and support preventive maintenance to improve the machine life [14].

Laghari *et al.* [15] analyzed wear-particle shape and edge detail, demonstrating that morphological descriptors can be used to distinguish among different wear-particle forms. Additional analysis of the stored data is presented to characterize five edge-detail traits: smooth, rough, straight, serrated, and curved. At the same time, four form features were classified as regular, irregular, elongated, and circular.

Laghari *et al.* [16] studied wear-particle classification using shape features and compared multiple classifiers to evaluate the effectiveness of feature-based particle identification. In this study, three classification models—the Support Vector Machine (SVM), *k*-Nearest Neighbors (*k*NN), and Discriminant Analysis (DA) classifier—are trained using various shape features, such as the Histogram of Oriented Gradients (HOG), Rotation Scale Translation (RST) invariant features, solidity, aspect ratio, circularity, and Euler number, to identify wear particles.

Laghari *et al.* [17] proposed identifying wear particles by their shape attributes using computer-vision-based analysis, thereby reinforcing the importance of morphological features in automated classification. An image analysis system is developed to improve wear judgments by using six morphological attributes: particle size, shape, edge details, color, surface texture, and thickness ratio. Six particle types—severe sliding wear, cutting edge, non-metallic, fatigue, water, and fiber particles—are identified by extracting shape features using a variety of criteria.

III. Understanding Wear Particles

Tribology is the study of friction, wear, and lubrication. It provides the basis for understanding how microscopic wear particles are generated, transported, and analyzed to evaluate machine health. As surfaces in relative motion contact under load, wear particles are continuously formed. This process first produces a "running-in" increase in particle generation. It then settles into a steady-state release rate. Changes in particle morphology in response to operating parameters (such as load, speed, and lubricant quality) provide important insights into new wear modes. Automated image-analysis systems use these characteristics to predict failure modes. This reduces reliance on expert judgment and supports proactive maintenance [18].

Tribology is the multidisciplinary study of friction, wear, and lubrication in interacting surfaces under relative motion. Wear-particle analysis is one of its important diagnostic applications. Tribology's economic and environmental importance demonstrates that wear and friction losses account for a substantial share of global energy expenditure [19].

Raadnui reviewed the use of wear-particle analysis and quantitative computer image analysis for machine condition monitoring. The study highlighted the importance of Ferrography for identifying wear mechanisms through particle morphology, including particle size, shape, color, texture, and concentration. The review also emphasized that computer-based image analysis can improve the objectivity and consistency of wear-particle classification compared with manual microscopic inspection [20].

This research investigates gearbox condition monitoring using both direct-reading and analytical Ferrography. A graphical user interface was developed to analyze wear particles in lubricating oil, helping detect wear severity and wear mechanisms at an early stage. The system supports maintenance decision-making, reduces breakdown costs, and improves gearbox reliability and availability [21].

Alternatively, SEM, often used in conjunction with Energy-Dispersive X-ray Spectroscopy (EDS), produces high-resolution images and elemental composition data for in-depth diagnostics of wear modes. Optical Microscopy (OM) provides a quick overview of particle populations. SEM provides high-resolution images. It also provides elemental composition when combined with EDS. However, SEM is more time-consuming and expensive than optical microscopy. Optical microscopy provides less detail. However, it enables faster imaging of larger sample sets. It is also sufficient for most morphological classifications.

Researchers standardize wear particle characterization around six primary morphological attributes: size (particle dimensions or Feret diameter), profile (shape) (outline descriptors: circularity, elongation), edge detail (sharpness, corner detection), color (optical appearance under transmitted or reflected light), thickness ratio (height-to-width aspect ratio), and surface texture (roughness, patterns). These attributes are extracted through image processing (segmentation, edge detection, and feature extraction) and used as inputs for rule-based or machine-learning classifiers [22].

Based on their shape and edge detail, profiles are frequently classified as regular (symmetrical, smooth), irregular (complex outlines), round, or elongated. For instance, abrasive wear produces uneven, angular particles, while fatigue-induced particles tend to be elongated with smooth edges. Color distinctions further improve diagnostics (e.g., dazzling metallic flakes vs. dark metallic oxides).

Different wear processes leave distinctive morphological characteristics that can be used to connect morphology to wear mechanisms:

- Rubbing wear creates polished, smooth particles with slight variations in texture.
- Severe sliding wear particles are large, flat, and often deformed particles produced when two metal surfaces slide heavily against each other under high load or poor lubrication, leading to plastic deformation and material shearing.
- Cutting wear particles are sharp-edged, elongated particles produced when a more rigid surface or abrasive particle cuts or gouges material from a softer metal surface, similar to a machining or plowing action.
- Fatigue Wear produces lengthy, layered particles that frequently exhibit patterns of concentric cracks.
- Chunky wear particles are large, irregularly shaped particles that result from the mechanical fracture or spalling of surface material, usually from gear teeth, bearings, or other load-bearing components under high stress or fatigue conditions.
- Spherical wear particles are globular, ball-shaped particles generated primarily due to adhesive wear or localized overheating, where small fragments of material melt and then rapidly cool and solidify into spherical shapes.

IV. Operating Procedures

The automated wear-particle software uses a multi-window, hierarchical, and interactive graphical interface. This interface controls both the Quantimet Q500MC hardware and the QWin image analysis toolkit. QWin is a modular image-processing and analysis software package for quantitative analysis tasks, including particle shape and size analysis. The analysis system is a commercial product developed by Leica Microsystems, not an in-house tool. This interface controls microscope parameters (illumination, magnification), camera settings, and image-analysis macros. It enables automated acquisition and processing without manual intervention. The interface seamlessly coordinates microscope imaging, image capture, segmentation, and feature extraction [23].

All images were acquired using the Quantimet Q500MC image analysis system and QWin software. Grayscale wear-particle images were recorded at a resolution of 768×576 pixels with 8-bit depth (256 gray levels). Illumination and microscope magnification were kept fixed for all samples. After acquisition, each field of view was converted to grayscale when necessary. The images were stored in uncompressed format to avoid detail loss before segmentation and Fourier analysis.

Grayscale images of particles are acquired via a Charged-Couple Device (CCD) camera and stored in the PC's memory, where thresholding converts 256-level images into binary masks, simplifying object extraction. A custom raster-scan boundary detection routine (utilizing the Sobel operator) then identifies contour transitions by comparing adjacent scan lines, yielding initial boundary coordinates.

The Sobel operator is a simple and widely used gradient-based edge detector, known for its ability to balance computational efficiency and noise reduction, which is particularly beneficial in applications such as wear particle monitoring [24].

Fig. 1 shows one such example. A set of particle images is captured and thresholded to convert them into a binary image, and profile images are the result of applying the Sobel edge detector operator. This edge detector was selected because it balances computational simplicity with edge localization performance. It is particularly effective for grayscale images, where clear contrast between particles and background enables accurate contour detection without requiring more complex operators.

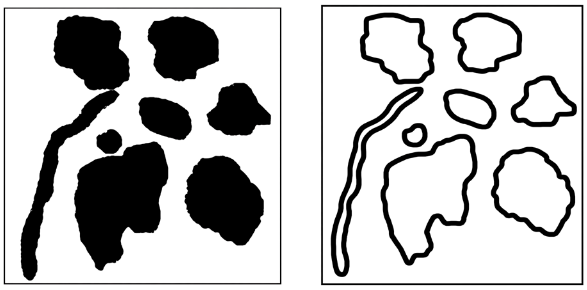

(a) (b)

Fig. 1. (a) Binary and (b) profile images of wear particles.

For reproducible contour analysis, the boundary of each segmented particle was parameterized as a closed curve and resampled to 256 equidistant points along the arc length. This fixed sampling rate ensures consistent contour length. As a result, all Fourier descriptors are computed from contours of identical length in the discrete domain. This process is independent of the original image resolution and particle size.

V. Fourier Descriptors

The three Fourier descriptors used for this investigation are briefly mentioned here:

A. Radial Fourier Descriptor

Radial Fourier Descriptors (RFDs) are Fourier-based shape descriptors. They represent a 2D object by measuring the radial distance from the center point to the boundary as a function of angle. This method is beneficial when shapes are more easily defined in polar coordinates than in Cartesian (XY) coordinates.

The descriptor chooses a reference point, typically the centroid of the shape. To convert the boundary points to polar coordinates, apply the following formula to each boundary point.

$$r_n = \sqrt{(x_n - x_c)^2 + (y_n - y_c)^2}$$

The angle between the point and the x-axis is defined by θ_n. The $r(\theta)$ is defined as the radius of the function of angle. To ensure uniform angular sampling, the boundary is interpolated so that $r(\theta)$ is measured at evenly spaced angles.

A 1-D Discrete Fourier Transform is applied to $r(\theta)$ to obtain the Radial Fourier descriptors as follows:

$$R_k = \frac{1}{N}\sum_{n=0}^{N-1} r_n \cdot e^{-2\pi ikn/N}$$

where R_k represents the Fourier coefficients.

Fig. 2 illustrates the distance from the centroid to the profile boundary coordinates. Each distance value is plotted against its corresponding angle (0° to 360°). Where (x_n, y_n) represents the center position of the profile calculated as the mean of n, and (x_c, y_c) represents a profile boundary point.

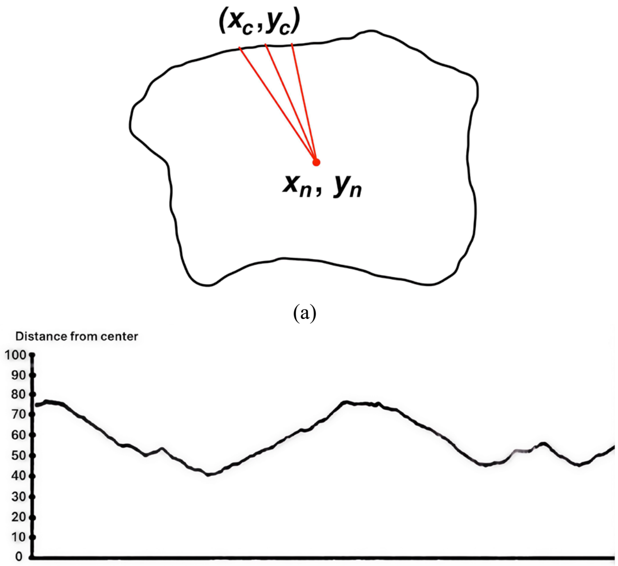

(a)
(b)

Fig. 2. The distance from the center representation of the particle profile using the Radial descriptor. (a) The original profile with its centroid; (b) the radial distance sequence along the contour points.

The first-harmonic approximation yields a circle, which differs considerably from the original profile. As more harmonics are added, up to eight, the Fourier approximation becomes closer to the original profile. The empirical testing was stopped at eight harmonics because it showed minimal improvement beyond this point. Higher-order harmonics increased computational cost but did not significantly improve shape reconstruction for most particles in our dataset.

In this study, the radial distance function $r(\theta)$ was sampled at 256 evenly spaced angles, and a 1-D Discrete Fourier Transform was applied. For all experiments, Radial Fourier descriptors were truncated at the 8th harmonic ($k = 0, \ldots, 8$). Preliminary tests with higher-order harmonics showed negligible improvement in shape reconstruction and clustering performance, while increasing computational cost; therefore, we adopted $k_{max} = 8$ as a fixed truncation rule.

However, with harmonics up to 8, the radial Fourier descriptor struggles to outline the concave parts of the profile. Therefore, the radial representation is insufficient for accurately describing irregular profiles [13].

B. Theta Fourier Descriptor

A Theta Fourier descriptor is a shape representation method in which the boundary of a shape is expressed as a function of the angle (θ). This angular function is then analyzed using a Fourier Transform to extract shape features. Unlike Radial Fourier descriptors, which primarily focus on radius variation, Theta descriptors characterize other boundary properties, such as curvature or tangent angle, in terms of θ or arc length.

The curvature, denoted as $k(\theta)$, and the tangent angle, $\phi(\theta)$, describe how the boundary "turns" as it is traversed. Applying the Fourier Transform to these functions yields descriptors that capture local shape characteristics, such as corners, symmetry, and recurring contour patterns. This makes Theta descriptors more sensitive to localized features than Radial descriptors.

Fig. 3 illustrates angular measurements of a profile boundary using the curvature method. Each boundary point has an associated angle, determined by the position of the next point relative to the preceding one. For example, the angular representation of a perfect circle is a straight line, while a square has an angle of 0° along its edges, increasing sharply to 90° near the corners.

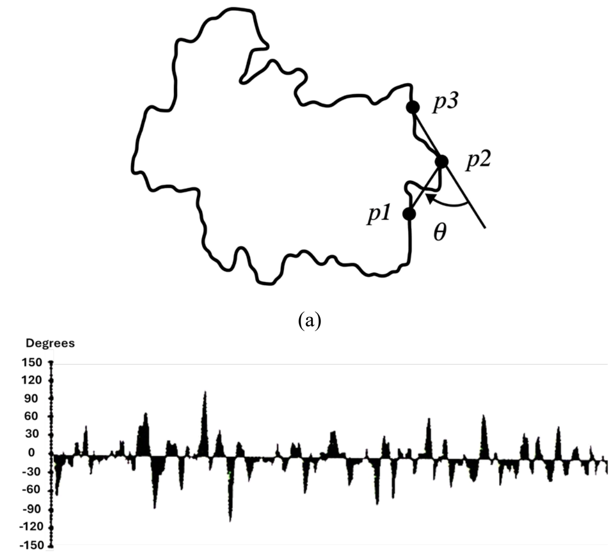

(a)
(b)

Fig. 3. An angular profile representation of a particle boundary using the Theta Fourier descriptor, illustrating curvature-based measurement at each contour point. (a) Angular profile representation; (b) curvature-based measurement along the contour points.

The reconstructed Theta Fourier outline approaches the original profile as the number of harmonics increases. Irregularities in the angular representation may cause a small break in the reconstructed contour, but this can be minimized by using a higher harmonic count—commonly around 21 [12].

The curvature-based angular function $k(\theta)$ was sampled at 256 points over 0–2π. Its Fourier series representation was truncated at the 21st harmonic (k = 0, …, 21). This upper limit was selected after an empirical evaluation that indicated that additional harmonics only marginally changed the reconstructed contour and did not improve cluster separation.

Although effective for both regular and irregular profiles, the non-smooth nature of angular representation often requires a large number of harmonics to accurately reproduce the shape.

C. XY Fourier Descriptor

The XY Fourier descriptor is obtained by applying the Fourier transform to the spatial boundary coordinates of a shape. It is mainly used in shape analysis and object recognition.

A 2D shape (generally a closed curve or border) is represented by a sequence of XY points in the plane, commonly known as a contour representation. Subsequently, the XY points are often turned into a complex sequence. For example, a boundary point (x = 4, y = 3) would be represented as a complex number $z = 4 + 3i$. The entire boundary becomes a sequence of such complex numbers.

Therefore, this set of complex coefficients, which describes the frequency domain shape, is obtained by applying a Discrete Fourier Transform (DFT) to the complex sequence. Lower-frequency coefficients describe the general shape (e.g., orientation, elongation), while higher-frequency coefficients capture finer details.

Using only a subset of these descriptors, such as the first few, can simplify or compress shapes. Furthermore, by properly normalizing them, Fourier descriptors can be rendered invariant to translation, scaling, rotation, and the beginning point of the contour. This is essential for consistent shape comparison.

Every point on the profile is defined by (x, y), representing the coordinates in the image plane that correspond to the spatial directions. Any point in the digital image has eight neighbors (vertical, horizontal, and diagonal). Each point has a unique set of values (x, y). The value of x or y of a given point is related to any of its neighbors by the addition or subtraction of 0 or 1. Consequently, the functions that describe the profile in terms of x and y separately are very smooth compared to the Theta representation.

Therefore, it is developed by computing the two parameters (x, y) separately, which enables the use of a 1D Fourier series algorithm to compute a 2D profile. This approach saves considerable computation time, and the x and y coefficients can be normalized by combining them into a single coefficient, which can then be used to classify profiles. Additionally, it can accurately outline 2D profiles using only a few harmonics.

The XY Fourier descriptor usually represents a smooth profile outline adequately after eight harmonics. The more irregular a profile is, the more accurately its harmonics must outline it. However, eight harmonics are usually sufficient, and regular profiles can be outlined with fewer than eight harmonics.

For the XY Fourier descriptor, the particle boundary was represented as a complex sequence:

$$z_n = x_n + iy_n, n = 0, \dots, N-1$$

sampled at 256 equidistant contour points. A 1-D DFT was applied separately to the x and y coordinates, and descriptors were truncated at the 8th harmonic. Thus, each particle was represented by the normalized coefficients Cc1–Cc8, corresponding to the selected harmonics k = 1–8. This fixed truncation rule was used consistently for all clustering experiments.

Note: details of the three descriptors can be found in Refs. [12, 13].

VI. Cluster Analysis Methodology

A. Feature Representation Using Fourier Descriptors

Fourier descriptors provide an effective mathematical framework for representing wear-particle morphology in a quantitative and invariant form. The descriptors transform particle boundaries into normalized coefficients. These coefficients capture essential geometric characteristics and remain invariant to translation, rotation, and scaling. These properties make the descriptors suitable for wear-particle analysis because particle orientation, size, and contour complexity can vary considerably. In the present study, Radial, Theta, and XY Fourier descriptors were employed to generate feature vectors for each particle, thereby enabling a systematic comparison of shape characteristics across different wear types.

In the context of wear-particle analysis, lower-order Fourier coefficients describe general morphological characteristics such as elongation and circularity. In contrast, higher-order coefficients capture finer contour details, including irregularities and edge roughness. These descriptors provide a compact and informative representation of particle shape. They also form the basis for the subsequent clustering analysis. This approach facilitates grouping particles by their morphological features, thereby aiding the identification of wear mechanisms.

B. Hierarchical Clustering Strategy

Hierarchical cluster analysis was used as the primary analytical framework to classify particles by morphological similarity. Hierarchical clustering may be implemented using either an agglomerative or a divisive strategy. In agglomerative clustering, each particle initially forms its own cluster, and clusters are progressively merged based on similarity until all particles belong to a single cluster. In contrast, divisive clustering begins with all particles grouped together and then successively separates them into smaller subgroups [25].

Using feature vectors derived from these descriptors, clustering algorithms can group particles by morphological similarity. The agglomerative approach is practical for this purpose. In agglomerative clustering, each particle starts as its own cluster, and pairs of clusters are progressively merged based on similarity until a single cluster encompasses all particles. This process is often visualized using a dendrogram, which illustrates the hierarchy of cluster merges.

Stated differently, every case is initially regarded as a distinct cluster. Two cases are merged into a single cluster in the second step. The third phase involves either merging two more cases into a new cluster or adding a third case to the cluster that already has two cases. At each stage, new cases are added to the cluster, or pre-existing clusters are merged.

Divisive hierarchical clustering can be seen as the opposite procedure. It begins by grouping all cases into a single cluster, then splitting the cluster until there are as many clusters as there are cases. In other words, all cases are treated as a single cluster in the first step. In the second step, the cluster is split into two, effectively dividing the cases into two groups. The splitting process continues until the desired number of clusters is reached.

The agglomerative method is generally more practical. However, divisive hierarchical clustering was chosen in this study. It is more suitable for investigating particle clustering from one group to five groups. This direction aligns better with the objective than reducing 20 individual clusters to 5 groups.

Divisive clustering is also preferred because the objective was to start from a general class of wear particles and split them into specific subtypes. This top-down approach aligns better with the nature of wear particle diversification than bottom-up agglomerative methods.

C. Distance Measure and Linkage Criterion

The outcome of hierarchical clustering depends strongly on the choice of distance metric and cluster-combination method. In the present work, Euclidean distance was used as the similarity measure between particles in the normalized Fourier feature space. This metric quantifies the separation between two particles by computing the square root of the sum of squared differences between their corresponding feature values. Euclidean distance reflects overall geometric similarity, and it is also straightforward and interpretable. Therefore, it is suitable for clustering based on Fourier coefficient features.

After the pairwise distances were obtained, cluster formation was considered using standard linkage criteria, including single, complete, and average linkage. Average linkage was adopted in this study. It considers the average distance between all pairs of cases in two clusters and does not rely only on the nearest or farthest neighbors. This provides a more balanced basis for grouping particles and reduces the sensitivity of clustering results to isolated local similarities or outliers.

D. Selection of Wear Particles and Features

The selection of variables is an important aspect of cluster analysis because it directly determines the characteristics used to define the resulting groups. In the present investigation, 20 wear particles were selected to represent common morphological categories, including rubbing, severe sliding, cutting, fatigue, spherical, and chunky particles. This selection reflects typical wear conditions, where rubbing particles are more frequently observed under normal operation, whereas the presence of other particle types may indicate more severe wear mechanisms [26].

For clustering purposes, the particles were represented using Fourier-coefficient features derived from the Radial, Theta, and XY descriptors. The corresponding coefficient values are presented in Tables I–III, respectively. Specifically, Table I lists the Radial Fourier coefficients, Table II lists the Theta Fourier coefficients, and Table III lists the XY Fourier coefficients used for clustering. The invariant coefficient values corresponding to the first eight harmonics were used as the feature set for comparative analysis. This consistent feature representation enabled a fair evaluation of each descriptor formulation's ability to separate different wear-particle types.

TABLE I. RADIAL FOURIER COEFFICIENTS USED FOR CALCULATION

P. #	Tribologist Assessment	C1	C2	C3	C4	C5	C6	C7	C8
1	Rubbing	3.02	4.54	2.54	1.51	1.34	1.38	0.47	0.28
2	Rubbing	21.25	0.64	2.1	0.64	0.73	0.32	0.39	0.35
3	Rubbing	0.92	8.77	2.81	3.29	1.84	0.74	0.58	0.74
4	Rubbing	4.33	9.44	8.43	0.58	6.21	4.72	1.47	2.26
5	Rubbing	2.41	8.03	2.78	8.84	3.86	1.74	2.01	1.14
6	Rubbing	0.94	3.05	2.62	1.88	0.84	1.07	0.55	0.56
7	Rubbing	1.36	2.84	6.57	3.34	0.59	1.52	1.16	0.87
8	Rubbing	5.61	14.42	5.35	1.9	2.22	2.05	1.98	1.12
9	Severe Sliding	3.05	34.01	3.45	1.16	4.23	2.58	1.28	0.2
10	Severe Sliding	3.39	19.83	8.04	2.52	3.28	1.8	2.47	1.48
11	Severe Sliding	3.56	31.25	5.69	0.57	0.47	0.38	0.09	0.04
12	Severe Sliding	0.51	14.24	1.93	3.12	1.72	0.74	1.89	0.52
13	Cutting	1.38	35.37	4.09	2.84	1.64	3.95	1.32	0.72
14	Cutting	0.64	43.8	0.46	0.59	0.18	4.56	0.18	0.31
15	Cutting	1.65	51.64	0.49	0.19	1.10	5.02	0.05	0.25
16	Fatigue	10.05	31.54	3.08	3.09	3.39	4.48	3.33	2.04
17	Fatigue	4.84	13.58	8.11	4.82	3.94	4.74	5.35	1.25
18	Spherical	0.51	0.49	0.33	0.24	0.08	0.12	0.04	0.1
19	Spherical	0.48	0.52	0.16	0.55	0.11	0.09	0.08	0.06
20	Chunky	1.0	5.14	2.57	1.36	1.29	0.77	0.78	0.38

TABLE II. THETA FOURIER COEFFICIENTS USED FOR CALCULATION

P. #	Tribologist Assessment	C1	C2	C3	C4	C5	C6	C7	C8
1	Rubbing	4.08	2.14	1.91	4.57	3.47	3.73	1.44	0.83
2	Rubbing	0.57	3.48	1.05	0.31	3.01	1.08	2.99	2.23
3	Rubbing	3.28	1.94	1.56	4.41	1.41	0.54	2.31	1.51
4	Rubbing	0.19	0.63	0.74	0.35	0.51	0.49	0.54	0.93
5	Rubbing	0.25	0.43	0.56	0.81	0.7	0.26	0.77	0.44
6	Rubbing	3.15	5.45	2.26	3.61	7.52	2.02	3.62	6.75
7	Rubbing	2.68	4.05	7.40	4.32	1.05	0.71	2.23	3.43
8	Rubbing	1.55	1.64	1.77	1.73	1.18	1.02	1.45	2.82
9	Severe Sliding	0.74	2.55	1.67	0.38	1.45	0.82	1.74	1.11
10	Severe Sliding	1.35	0.81	0.73	0.51	1.33	0.57	1.17	0.78
11	Severe Sliding	1.03	1.68	2.07	2.18	1.21	0.52	1.81	0.78
12	Severe Sliding	0.36	0.97	1.17	1.45	0.76	0.28	0.89	0.29
13	Cutting	1.57	4.05	0.55	1.38	1.87	0.65	1.28	1.98
14	Cutting	0.39	2.03	0.28	1.32	0.22	1.77	0.23	2.38
15	Cutting	0.2	1.28	0.15	1.28	0.09	0.92	0.14	1.08
16	Fatigue	0.36	0.27	0.98	0.98	0.06	0.15	0.65	1.41
17	Fatigue	0.67	0.37	0.33	0.47	0.18	0.62	0.37	0.75
18	Spherical	0.35	0.92	0.43	0.54	0.79	0.43	0.11	0.08
19	Spherical	0.16	0.03	0.49	0.06	0.27	0.19	0.17	0.16
20	Chunky	0.51	0.66	0.5	0.92	1.01	0.78	1.74	1.42

TABLE III. XY FOURIER COEFFICIENTS USED FOR CALCULATION

P. #	Tribologist Assessment	Cc1	Cc2	Cc3	Cc4	Cc5	Cc6	Cc7	Cc8
1	Rubbing	21.26	1.97	1.13	0.38	0.93	0.53	0.27	0.30
2	Rubbing	21.27	0.63	2.09	0.64	0.73	0.31	0.38	0.35
3	Rubbing	21.33	1.23	1.77	0.92	0.84	0.36	0.37	0.23
4	Rubbing	17.46	1.45	0.27	0.57	0.5	0.71	0.48	0.23
5	Rubbing	23.39	1.24	2.0	0.96	0.89	0.6	0.33	0.25
6	Rubbing	20.81	1.64	1.55	1.24	0.87	0.48	0.58	0.24
7	Rubbing	18.15	3.34	1.43	1.33	1.38	0.65	0.67	0.52
8	Rubbing	17.24	3.06	2.82	1.21	0.88	0.74	0.59	0.54
9	Severe Sliding	18.86	1.55	2.69	0.51	1.18	0.78	0.23	0.31
10	Severe Sliding	21.01	1.93	1.74	0.84	0.44	0.71	0.38	0.34
11	Severe Sliding	21.45	1.86	2.29	0.6	0.59	0.16	0.14	0.19
12	Severe Sliding	22.87	0.54	1.72	0.45	0.47	0.58	0.24	0.34
13	Cutting	18.84	0.9	1.91	0.9	0.92	0.4	0.52	0.27
14	Cutting	20.34	1.27	12.27	0.11	0.82	0.03	0.43	0.02
15	Cutting	21.74	1.43	2.38	0.31	0.74	0.14	0.47	0.10
16	Fatigue	15.52	2.22	1.8	0.76	0.49	0.48	0.75	0.63
17	Fatigue	10.67	1.6	1.53	1.12	0.72	0.52	0.83	0.68
18	Spherical	23.81	0.51	0.26	0.23	0.28	0.05	0.05	0.07
19	Spherical	26.91	0.24	1.58	0.12	0.15	0.04	0.15	0.03
20	Chunky	23.30	0.98	1.04	0.66	0.65	0.5	0.14	0.21

E. Methodological Framework for Comparative Evaluation

The overall methodological framework of this study combines invariant shape representation with hierarchical clustering to evaluate the discriminative ability of different Fourier Descriptor formulations. First, particle contours were represented numerically using Radial, Theta, and XY Fourier coefficients. Next, hierarchical clustering was applied using Euclidean distance and average linkage to group particles according to morphological similarity. Finally, the clustering behavior produced by each descriptor type was compared to determine which representation most effectively supports wear-particle classification.

This structured methodology provides an objective basis for examining the grouping behavior of wear particles and for assessing the suitability of alternative descriptor formulations for morphological classification. The framework separates feature extraction, clustering strategy, and comparative evaluation. This improves clarity. It also supports reproducible analysis.

Having established the feature representation, clustering strategy, distance measure, linkage criterion, and comparative evaluation framework, the next section presents the clustering results obtained from the Radial, Theta, and XY Fourier descriptors. It discusses their effectiveness in distinguishing among different wear-particle morphologies.

VII. RESULTS AND DISCUSSION

Based on the methodological framework described in the previous section, hierarchical clustering was applied to the Fourier descriptor feature sets to assess how effectively each descriptor groups wear particles by morphological similarity.

This clustering approach helps distinguish between benign and active wear particles. It also enables early detection of abnormal wear conditions. Such analysis reduces reliance on expert interpretation and enhances the objectivity and efficiency of wear particle classification.

Integrating descriptors with hierarchical clustering provides a robust framework for classifying wear particles based on morphology. This method captures essential shape features and groups particles in a manner that reflects underlying wear mechanisms. Automating the classification process enhances the reliability of wear diagnostics and supports proactive maintenance strategies.

Several additional aspects were determined after selecting the clustering technique. These aspects included the variables used in the analysis, the distance measure between cases, and the cluster-combination method.

Selecting the variables to include in cluster analysis is always important, as it determines the characteristics of the defining groups. The 20 particles used in the experiment are presented for cluster analysis using the Radius, Theta, and XY Fourier coefficient descriptor features, as shown in Tables I–III, respectively. The invariant "C" coefficient features for the 1st eight Fourier harmonics are described from the 3rd to the 10th column.

A. Dendrogram-Based Analysis of Fourier Descriptor Clustering

The clustering results reveal clear differences in the ability of the three Fourier descriptor formulations to distinguish among wear-particle types. The dendrograms in Fig. 4(a)–(c) show that each descriptor captures different aspects of particle morphology, leading to variations in cluster compactness, separation, and overlap.

Each leaf at the bottom represents one of the 20 wear particles (P1 to P20). The vertical lines represent mergers between particles or clusters. The height (y-axis) of each merge represents the Euclidean distance between the merged clusters in the normalized Fourier feature space. Clusters that merge at lower heights are more similar in shape characteristics; those that merge at higher heights are more different.

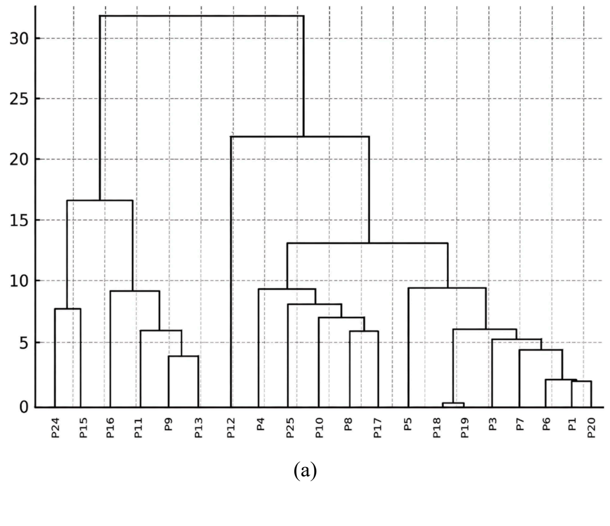

(a)

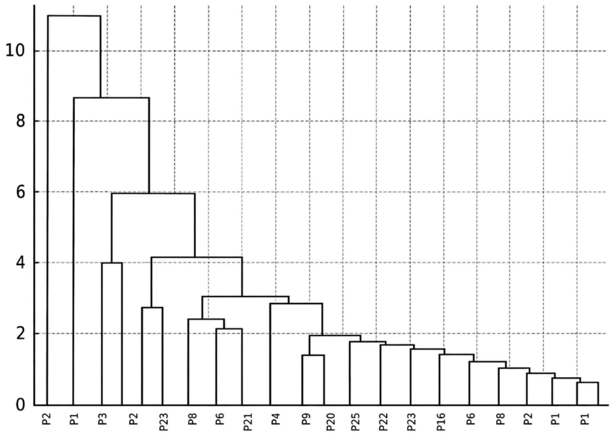

(b)

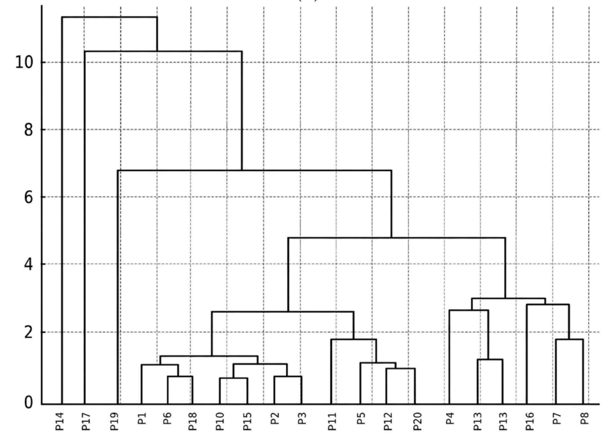

(c)

Fig. 4. Dendrograms obtained from hierarchical clustering of wear particles using three different Fourier Descriptor formulations: (a) Radial Fourier coefficients, (b) Theta Fourier coefficients, and (c) XY Fourier coefficients.

As shown in Fig. 4(a)–(c), the three Fourier descriptor formulations produce noticeably different clustering patterns for the wear particles. Each dendrogram illustrates the clustering structure of the 20 wear particles in the normalized feature space, where the linkage height represents the Euclidean distance between merged clusters. Lower linkage distances indicate greater morphological similarity, whereas higher linkage distances reflect stronger separation among particle groups.

1) Radial fourier descriptor dendrogram

The dendrogram based on the Radial Fourier descriptor in Fig. 4(a) provides only moderate discrimination among particle types. Rubbing particles tend to cluster at relatively low linkage distances. However, overlap remains apparent between rubbing and severe sliding particles. This indicates that the radial representation is less effective for irregular or concave profiles.

The Radial dendrogram shows that rubbing particles (P1–P8) converge at exceptionally short distances, indicating that the descriptor accurately reflects their smooth, rounded contours. Nonetheless, severe-sliding particles (P9–P12) are not reliably distinguished from rubbing particles, indicating that radial descriptors struggle to distinguish between these two wear types due to overlapping contour distances.

Cutting particles (P13–P15) establishes an independent group. However, the separation occurs at greater linkage distances, indicating limited discriminative capacity. Fatigue particles (P16–P17) exhibit moderate distinction while retaining some resemblance to rubbing particles. Spherical (P18–P19) and chunky particles (P20) amalgamate in later stages, indicating their distinctiveness relative to other wear types. Radial descriptors effectively represent the overall elongation of a form but are inadequate for intricate or concave profiles.

Therefore, Radial clustering reveals some groupings of particles with analogous characteristics; nonetheless, overlaps are prevalent. For instance, rubbing particles tend to amalgamate early, but particles subjected to intense sliding and cutting are not distinctly separated. Radial descriptors effectively capture elongation and overall contour changes; however, they are inadequate for irregular or concave profiles, resulting in diminished separation performance.

2) Theta fourier descriptor dendrogram

The Theta Fourier descriptor dendrogram in Fig. 4(b) shows improved sensitivity to angular and localized contour variations. In particular, cutting particles exhibit clearer grouping due to their sharp and elongated boundaries. However, some ambiguity is still observed between rubbing and severe sliding particles, suggesting that angular information alone is insufficient for complete class separation.

The Theta dendrogram categorizes particles according to angular variation at their peripheries. Cutting particles (P13–P15) exhibit strong clustering due to their sharp, elongated profiles, which generate distinctive angular fingerprints. Spherical particles (P18–P19) remain distinct until the last stages, as their nearly uniform angular profile differs from other wear types. Rubbing particles (P1–P8) amalgamate with severe sliding particles (P9–P12), exhibiting similarities in local angular characteristics and resulting in mixed clusters.

Fatigue particles (P16–P17) occupy an intermediary location, exhibiting irregular angular transitions that partially coincide with both cutting and sliding types. The Theta descriptor is more responsive to localized features, such as corners and curvature. However, this sensitivity can lead to overlap when different wear types have similar angular fluctuations.

The Theta-based dendrogram, therefore, exhibits slightly better performance because of its heightened sensitivity to angular deviations and localized contour alterations. Specific clusters exhibit distinct separation of cutting particles due to their acute angles and elongated characteristics. Nonetheless, ambiguity persists between the rubbing and severe sliding categories, as the distinction between smooth and slightly distorted objects converges in angular space.

3) XY fourier descriptor dendrogram

By contrast, the XY Fourier descriptor dendrogram in Fig. 4(c) provides the clearest and most compact clustering structure. Rubbing particles form a closely grouped cluster, while cutting, fatigue, spherical, and chunky particles exhibit more distinct separation than in the other two descriptor spaces. This result indicates that the XY Fourier descriptor captures both global shape characteristics and local profile irregularities more effectively, making it the most suitable representation for wear-particle classification in the present study.

The XY dendrogram offers the most lucid and discriminative clustering. The rubbing particles (P1–P8) form a compact, closely knit cluster, highlighting their uniform smoothness and symmetry. Cutting particles (P13–P15) exhibit a unique clustering at elevated levels owing to their elongated, slender shapes. Spherical particles (P18–P19) stay distinct until the final stages due to their morphologically unique circular borders.

The chunky particle (P20) is separated later, indicating its irregular, fragmented shape. Fatigue particles (P16–P17) constitute a separate subgroup that merges with other clusters at intermediate distances, consistent with their irregular, albeit less severe, appearance. Significantly, severe-sliding particles (P9–P12) exhibit partial separation while remaining in proximity to rubbing particles, a phenomenon anticipated due to their flat yet elongated characteristics. The XY descriptor consequently generates compact, distinctly separated clusters, surpassing Radial and Theta in their ability to differentiate wear mechanisms.

The XY dendrogram offers the most precise and distinct categorization of wear particles. Rubbing particles create dense, closely-knit clusters, indicative of their smooth, uniform shapes. Cutting particles aggregate at moderate distances, aligning with their slender, elongated shapes. Spherical and chunky particles remain separate until late mergers, visibly confirming their morphological individuality. Fatigue particles aggregate in the interstices, exhibiting intermediate resemblance to uneven wear patterns. The XY descriptor captures both global smoothness and local imperfections. This makes it superior for clustering.

4) Distance measurement

Distance is the separation between two points or objects. These concepts are essential in cluster analysis, as particles are grouped based on similarity. An everyday use of distance measurement is the Euclidean distance, defined as the square root of the sum of squared differences between the values of the clustering variables.

For example, the distance between cases X & Y can be calculated as:

$$Dis(x, y) = \sqrt{\sum_{i}^{n} (X_i - Y_i)^2}$$

where *n* represents the total number of features being used: in this case, eight features.

The 20 wear-particle images used in the clustering experiment are shown in Fig. 5, representing rubbing, severe sliding, cutting, fatigue, spherical, and chunky particle types.

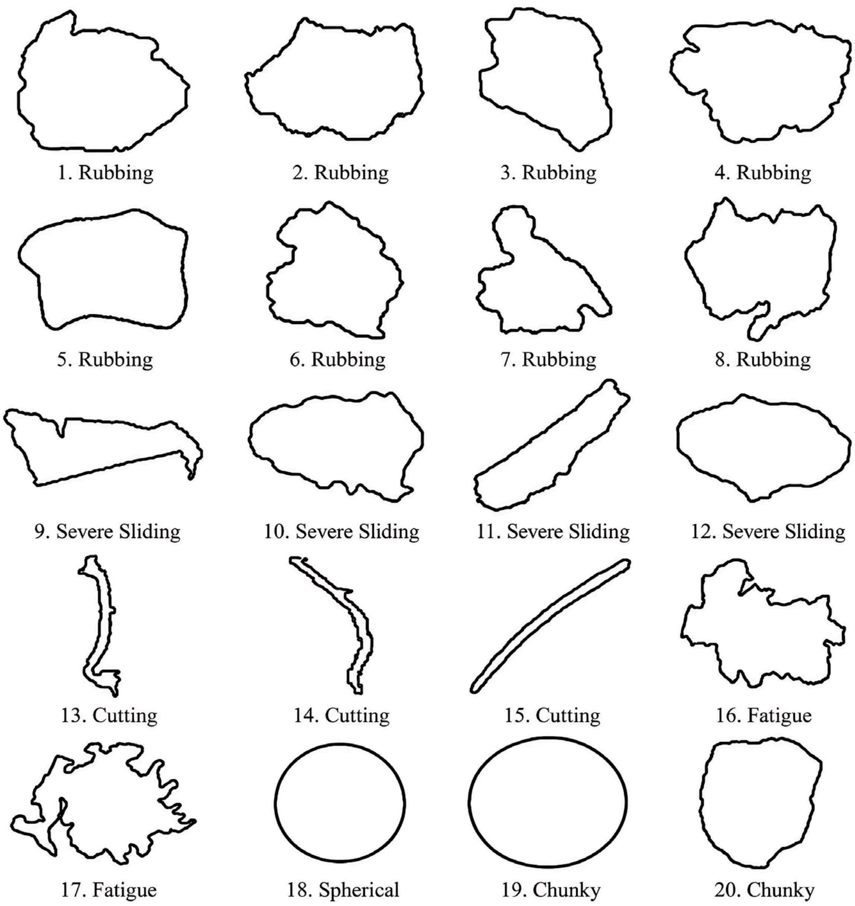

Fig. 5. Images of six types of wear particles.

5) Combining methods

After distance measurements for all cases are obtained, the combination can be performed using complete, single, or average linkage. In complete linkage, or the furthest neighbor technique, the distance between two clusters is calculated as the distance between the two furthest cases. In the single-linkage method, also known as the nearest-neighbor method, the distance between two clusters is calculated as the distance between the two nearest cases.

In average linkage, the distance between two clusters is defined as the average of the distances between all pairs of cases. For example, if case q and case 2 form cluster X and cases 3–5 form cluster Y, the distance between clusters X & Y is taken to be the average of the distances between the following pairs of cases (1, 3) (1, 4) (1, 5) (2, 3) (2, 4) and (2, 5). The average linkage method was used to incorporate information from all pairs of distances, not just the nearest or farthest.

B. Comparative Discussion of Wear Particle Classification

The clustering results demonstrate clear differences in the ability of the three Fourier Descriptor formulations to distinguish among wear-particle types. Dendrogram analysis shows that each descriptor captures distinct aspects of particle morphology, resulting in variations in cluster compactness, separation, and overlap.

Table IV presents the classification of 20 particles using the Radial, Theta, and XY Fourier features in comparison with the Tribologist's assessment. The Fourier Descriptor clustering has been shown to effectively group the 20 particles into three to five clusters, corresponding to the five distinct types of wear.

The results indicate some overlap of profile parameters between different wear types, and there is a significant difference in the performance of the three descriptors. There are many reasons for this, the primary one being that particles with the same identity differ in their profiles. For example, particle number 7 cannot be differentiated from the rubbing particles, although the expert rated it as severe sliding.

Another approach to the problem is to identify global or local characteristic features for each particle type, and then select descriptors that capture these features. Therefore, the first step is to examine the 20 particles in terms of their profile characteristics and identify the most suitable descriptor for distinguishing them. Hence, by looking at these particles, the following points summarize what the particle profile provides for classifying wear particle types:

(1) Cutting particles have an extended, thin profile and can be identified and distinguished from the rest by the aspect ratio and area/perimeter ratio. For instance, XY Fourier Descriptor aspect-ratio features can be used to identify these particles.

TABLE IV. THE CLUSTER ANALYSIS RESULT USING THE THREE COEFFICIENT FEATURES

P. #	Tribologist Assessment	# of Clusters 5 Clusters R	T	XY	4 Clusters R	T	XY	3 Clusters R	T	XY
1	Rubbing	1	1	1	1	1	1	1	1	1
2	Rubbing	2	2	1	1	2	1	1	1	1
3	Rubbing	2	1	1	1	1	1	1	1	1
4	Rubbing	3	5	2	2	2	2	1	1	1
5	Rubbing	2	5	3	1	2	1	1	1	1
6	Rubbing	1	3	1	1	3	1	1	2	1
7	Rubbing	1	4	2	1	4	2	1	3	1
8	Rubbing	3	5	2	2	2	2	1	1	1
9	Severe Sliding	4	5	1	3	2	1	2	1	1
10	Severe Sliding	3	5	1	2	2	1	1	1	1
11	Severe Sliding	4	5	1	3	2	1	2	1	1
12	Severe Sliding	2	5	3	1	2	1	1	1	1
13	Cutting	4	2	1	3	2	1	2	1	1
14	Cutting	5	5	1	4	2	1	3	1	1
15	Cutting	5	5	1	4	2	1	3	1	1
16	Fatigue	4	5	2	3	2	2	2	1	1
17	Fatigue	3	5	4	2	2	3	1	1	2
18	Spherical	1	5	3	1	2	1	1	1	1
19	Spherical	1	5	5	1	2	4	1	1	3
20	Chunky	1	5	3	1	2	1	1	1	1

(2) Spherical particles can be easily identified using the roundness factor or XY Fourier Descriptor coefficient features, which have a significant value for the first feature and an exceptionally low value for the second and subsequent features.
(3) Fatigue particles typically exhibit a jagged, irregular profile. The XY Fourier deviation features can capture irregular particle profiles.
(4) Rubbing particles have a regular profile, whereas severe sliding and chunky particles can be confused with rubbing particles. Therefore, although important, distinguishing among Rubbing, Severe Sliding, and Chunky profiles does not seem satisfactory.

C. Clustering Performance Evaluation

Quantitative cluster validity measures further support these qualitative observations. The comparative evaluation using the Silhouette Score and Davies–Bouldin Index confirms that the XY Fourier descriptor consistently achieves superior clustering performance relative to the Radial and Theta descriptors. This finding highlights the effectiveness of the XY formulation as a compact and discriminative feature representation for automated wear-particle analysis.

The Silhouette Score ranges from −1 to 1, with higher values indicating better-defined clusters. In contrast, the DB Index measures intra-cluster similarity relative to inter-cluster separation, where lower values indicate better clustering.

Table V summarizes the performance of Radial, Theta, and XY Fourier descriptors across 3-, 4-, and 5-cluster configurations. The results show that the XY descriptor consistently yields the highest Silhouette Scores and the lowest DB Index values, supporting its superior discriminative power, as observed in the qualitative results.

The results emphasize the practical value of the proposed framework for condition monitoring. They also identify current dataset limitations. These limitations motivate future work using larger datasets and more advanced classification strategies.

According to a statistical comparison of the three descriptors (Table V), the XY Fourier descriptor consistently performs better than the Radial and Theta descriptors, producing the lowest Davies-Bouldin Index (0.679) and the greatest Silhouette Score (0.336). These measurements confirm the more compact and well-separated clusters produced by XY descriptors. Theta descriptors are marginally better than radial descriptors, especially when it comes to capturing angular variations. However, they are still not as good as XY at distinguishing among particle types. The qualitative clustering results shown in Table IV are consistent with this quantitative data.

TABLE V. PERFORMANCE OF RADIAL, THETA, AND XY FOURIER DESCRIPTORS

Descriptor	Silhouette Score ↑	Davies–Bouldin Index ↓	Best # of Clusters	Strengths	Weaknesses
Radial	0.283	0.726	3	Captures elongation & general contour	Fails on concave/irregular profiles; overlap between rubbing & sliding
Theta	0.301	0.710	3–4	Sensitive to angular features (corners, symmetry)	Ambiguity between rubbing & sliding; needs more harmonics
XY	0.336	0.679	4–5	Best separation; compact, distinct clusters; captures smooth & irregular profiles	Slight overlap between rubbing & severe sliding

The Radial values point to a moderate level of clustering quality. Better-defined clusters are typically indicated by a lower Davies–Bouldin index (closer to 0) and a higher silhouette score (closer to 1). A slight improvement in cluster separation and compactness is indicated by the values for Theta, which are marginally better than the radial coefficients. Compared to the findings from the radial and theta coefficients, the clustering results for XY are better. The clusters are less overlapping and more distinct in the XY descriptor space, as indicated by the lower Davies-Bouldin index and higher silhouette score.

D. Practical Implementation and Computational Perspective

From an implementation perspective, the proposed XY Fourier descriptor is computationally lightweight. Each contour was resampled to 256 points. The maximum harmonic order was set to $k_{max} = 8$. Under these conditions, descriptor extraction requires approximately 10^3–10^4 elementary arithmetic operations per particle. The resulting normalized coefficients require fewer than 100 bytes of storage. This operation count is compatible with sub-millisecond processing per particle. Such processing can be achieved on modern low-cost microcontrollers or Digital Signal Processors (DSPs) operating at tens of MHz. Therefore, the method can support real-time inspection of multiple wear particles per video frame. This makes it suitable for embedded condition-monitoring systems.

The present study focuses on unsupervised clustering to evaluate descriptor quality rather than on training a specific supervised classifier. For deep-learning integration, such as a CNN operating directly on raw wear-particle images, substantially larger labeled datasets are usually required. As a rule of thumb, robust CNN training for multi-class classification often demands at least an order of magnitude more labeled samples than are available in our current dataset, i.e., on the order of 104 labeled images overall or $\geq$ 103 examples per class, especially in the presence of class imbalance. In contrast, the XY Fourier descriptor provides a compact feature representation (tens of coefficients per particle) that can be effectively exploited by classical supervised models (e.g., SVMs, random forests) with more modest dataset sizes. A systematic comparison between CNN-based models and XY descriptor-based classifiers is an important direction for future work. Extended datasets should support such a comparison.

This research offers several contributions that distinguish it from earlier studies in wear-particle analysis and tribology:

1) Integration of fourier descriptors with cluster analysis

This study systematically uses three forms of Fourier descriptors (Radial, Theta, XY) to mathematically represent particle boundaries, in contrast to previous research that utilized shape features or texture analysis.

These descriptors are fundamentally invariant to translation, rotation, and scaling, thereby enhancing classification robustness compared to approaches that rely on raw images or manually generated features. By integrating hierarchical clustering, this study establishes an automated and quantitative classification pipeline. The pipeline reduces subjectivity compared with expert-based categorization.

In earlier works, Fourier descriptors were primarily used for particle-profile recognition and wear-particle profile analysis without an explicit unsupervised clustering stage [12, 13]. At the same time, other studies relied on hand-crafted geometric or texture features combined with rule-based systems or classifiers [4, 7, 15–17]. The present framework, therefore, closes the gap between descriptor-based representation and label-free particle grouping, enabling direct comparison of particle morphologies in an invariant feature space.

2) Comparative evaluation of descriptor performance

This study directly compares Radial, Theta, and XY descriptors. This differs from most previous studies, which used only one descriptor type.

The research demonstrates that XY Fourier descriptors excel at cluster separation, as confirmed by the Silhouette Score and Davies–Bouldin Index. This establishes a quantifiable standard for subsequent investigations in wear particle detection. Previous tribology studies typically focused on a single representation—such as radial concave deviation features [4], co-occurrence texture measures [7], or global shape descriptors [12,13] and reported only classification accuracy, making it difficult to assess which descriptor family is intrinsically most separable. By reporting side-by-side clustering quality across all three descriptor types, this work provides practical guidance for future systems that must balance discriminative power with computational and implementation costs.

E. Novelty and Limitations

The use of the Silhouette and Davies–Bouldin indices to evaluate clustering performance is relatively rare in tribology. This introduces an objective validation layer that goes beyond visual dendrogram analysis and subjective expert evaluation.

Earlier wear-particle studies evaluated performance either qualitatively—via visual inspection of dendrograms and micrographs—or through supervised metrics such as classifier accuracy and confusion matrices [1, 4, 7, 16], with little emphasis on unsupervised cluster validity indices. Adopting general data-mining measures such as the Silhouette and Davies-Bouldin indices [25] thus aligns wear particle analysis with best practices in clustering research. It provides a reproducible benchmark for comparing future algorithms.

Traditional Ferrography relies on specialist analysis, necessitating manual interpretation of particle morphology by microscopy.

This methodology combines image processing, Fourier analysis, and clustering into an automated system. The system reduces subjectivity, improves repeatability, and supports scalability for industrial monitoring. Classical wear-debris analysis and Ferrographic inspection rely heavily on specialist interpretation and rule-based judgment [18, 20, 21]. Recent deep-learning approaches require large, labeled datasets and substantial retraining effort [1, 5, 9–11]. In comparison, the proposed pipeline offers a more data-efficient route to automation. It can be integrated into existing image-analysis workflows to provide consistent, operator-independent screening of wear states while remaining interpretable in terms of physically meaningful shape descriptors.

Automated wear-particle analysis plays a critical role in condition monitoring and fault diagnosis; however, existing shape-based approaches suffer from two major limitations. First, commonly used Fourier descriptors—such as radial and curvature (Theta) descriptors—encode only partial geometric information, which can limit their ability to discriminate complex, asymmetric particle morphologies. Second, many recent studies rely on supervised machine-learning or deep-learning classifiers. The performance of these classifiers depends on large, well-balanced labeled datasets, which require substantial computational resources.

To address these challenges, this research adopts an unsupervised shape-analysis framework based on Fourier descriptors and systematically investigates the suitability of different descriptor formulations for wear-particle characterization. In particular, particle boundaries are represented using Radial, Theta, and XY Fourier descriptors, and their effectiveness is evaluated using standard clustering validity indices rather than classifier-dependent accuracy measures. This strategy enables an objective comparison of descriptor expressiveness while remaining applicable to small, partially labeled datasets.

The primary methodological innovation of this work is the evaluation of the XY Fourier descriptor. The results show that it provides superior discriminative capability. It performs better than radial- and theta-based descriptors under identical clustering conditions. Unlike prior studies that focus on either radial distance functions or curvature-based representations, the proposed approach exploits the joint spatial encoding of x–y coordinates, thereby improving cluster compactness and separation across diverse wear-particle shapes.

This study also emphasizes practical deployment. The proposed XY descriptor yields compact feature vectors with low computational complexity, making it well-suited for real-time embedded condition-monitoring systems. Moreover, its effectiveness in an extremely small-sample regime (20 labeled images across six classes) highlights its suitability for applications where large, annotated datasets required by deep-learning models are unavailable. Together, these contributions support the proposed framework as a robust, interpretable, and computationally efficient alternative to data-intensive learning-based approaches for wear-particle analysis.

F. *Dataset Limitations and Future Work*

The size and composition of the labeled dataset constrain the present study. Only 20 labeled wear-particle images are currently available. These images are distributed across six classes, corresponding to fewer than four labeled samples per class. This small sample size limits the use of fully supervised learning approaches. It also motivates the use of unsupervised clustering and descriptor-based evaluation. While the dataset is sufficient for comparative assessment of Fourier descriptor expressiveness, it does not support statistically robust training or validation of data-intensive classifiers such as convolutional neural networks.

Future work will focus on systematically expanding the dataset in two complementary directions. First, additional wear-particle images will be collected under controlled operating conditions to increase both intra-class variability and inter-class coverage, with a target of several hundred samples per class to support classical supervised classifiers (e.g., SVMs and random forests). Second, longer-term data acquisition campaigns are planned to build a substantially larger labeled dataset—on the order of 10^3 samples per class—to enable fair comparison with deep-learning-based models operating directly on raw images. Semi-supervised and weakly supervised labeling strategies will also be explored to reduce annotation effort. These strategies will use the proposed XY Fourier descriptor as a compact and interpretable feature representation.

VIII. Conclusion

The integration of Radial, Theta, and XY Fourier descriptors with hierarchical clustering provides a robust and practical framework for morphological classification of wear particles. This methodology enables quantitative, objective analysis by extracting key shape features and grouping particles into clusters that reflect the underlying wear mechanisms.

Fourier descriptors provide a compact and invariant representation of particle contours. They capture both global and local shape characteristics. Lower-order descriptors characterize general morphology, such as circularity and elongation. In contrast, higher-order descriptors represent finer details, including surface irregularities and texture, when used as input for hierarchical clustering.

Experimental results demonstrate that this approach can classify particles into three to five distinct wear types with consistency comparable to expert assessments. Average linkage and Euclidean distance were used in clustering. Together, they consider both overall similarity and subtle differences between particle shapes.

Some misclassifications occur due to variability among wear types. Others arise from morphological overlap and can be reduced by refining descriptor selection. The selected descriptors should emphasize features that are specific to each wear mechanism.

Although the labeled dataset was expanded to 20 wear-particle images, the sample size remains too small to assess the statistical stability of the clustering results. In this study, clustering validity indices are interpreted comparatively. They are used to evaluate the relative expressiveness of different Fourier descriptor formulations. All descriptors are evaluated under identical experimental conditions. The indices are not used to provide definitive estimates of the robustness of cluster structure.

Future work will address this limitation through systematic dataset expansion and simulated data augmentation. In particular, additional wear-particle images will be acquired to increase sample size and morphological diversity. At the same time, synthetic augmentation strategies—such as controlled perturbation of particle boundaries and variation of Fourier descriptor coefficients—will be employed to assess clustering sensitivity and stability under repeated trials. These steps will enable more rigorous statistical validation of clustering performance and robustness.

A small sample size and overlapping morphological profiles between certain wear types may affect the generalizability of the results.

The present work focuses on the design and comparative evaluation of Fourier descriptor-based shape representations under unsupervised clustering. Modern supervised classifiers, such as SVMs or CNNs, could improve particle-type discrimination. However, a rigorous comparison would require a larger and well-balanced labeled dataset. It would also require extensive hyperparameter tuning to avoid overfitting. Given that our dataset is only partially labeled and exhibits pronounced class imbalance, we restricted ourselves to unsupervised cluster validity measures to assess descriptor quality. Nevertheless, the proposed XY Fourier descriptor defines a compact, rotation-, translation-, and scale-normalized feature space that can be directly fed into SVMs, random forests, or CNN-based architectures. A systematic, supervised evaluation of XY descriptors versus raw images and alternative feature representations is an important avenue for future work.

Future work could explore real-time analysis using embedded systems. It could also expand the dataset to include hundreds of particles. Deep-learning models, such as CNNs and Vision Transformers, may improve classification accuracy, especially for complex and overlapping profiles.

The use of Silhouette and Davies-Bouldin indices further confirmed the superiority of the XY descriptor in producing compact and well-separated clusters.

Conflict of Interest

The authors declare no conflict of interest.

Author Contributions

Conceptualization, M.S.L.; Methodology, A.H.; Software, M.S.L.; Validation, M.H.; Formal Analysis, A.A.; Investigation, A.H. and A.W.; Resources, A.A.; Data Curation, A.W.; Writing—Original Draft, M.S.L.; Writing—Review & Editing, A.W. and M.H. All authors had approved the final version.

References

[1] L. He, H. Wei, and W. Gao, "Research on an intelligent classification algorithm of ferrography wear particles based on integrated ResNet50 and SepViT," *Lubricants*, vol. 11, no. 12, 530, 2023.

[2] N. K. Myshkin, O. K. Kwon, A. Y. Grigoriev *et al.*, "Classification of wear debris using a neural network," *Wear*, vol. 203, pp. 658–662, 1997.

[3] L. Zhu, X. Xiao, D. Wu *et al.*, "Qualitative classification of lubricating oil wear particle morphology based on coaxial capacitive sensing network and SVM," *Sensors*, vol. 22, no. 17, 6653, 2022.

[4] W. Yuan, K. S. Chin, M. Hua *et al.*, "Shape classification of wear particles by image boundary analysis using machine learning algorithms," *Mechanical Systems and Signal Processing*, vol. 72, pp. 346–358, 2016.

[5] P. Peng and J. Wang, "Wear particle classification considering particle overlapping," *Wear*, vol. 422, pp. 119–127, 2019.

[6] Q. Li, T. Zhao, L. Zhang *et al.*, "Ferrography wear particles image recognition based on extreme learning machine," *Journal of Electrical and Computer Engineering*, vol. 2017, no. 1, 3451358, 2017.

[7] G. P. Stachowiak, G. W. Stachowiak, and P. Podsiadlo, "Automated classification of wear particles based on their surface texture and shape features," *Tribology International*, vol. 41, pp. 34–43, 2008.

[8] T. Wu, Y. Peng, S. Wang *et al.*, "Morphological feature extraction based on multiview images for wear debris analysis in on-line fluid monitoring," *Tribology Transactions*, vol. 60, no. 3, pp. 408–418, 2016.

[9] J. You, S. Fan, Q. Yu *et al.*, "Real-time ferrogram segmentation of wear debris using multi-level feature reused UNet," *Sensors*, vol. 24, no. 8, 2444, 2024.

[10] L. He, H. Wei, and C. Sun, "TCBGY net for enhanced wear particle detection in ferrography using self attention and multi scale fusion," *Scientific Reports*, vol. 14, no. 1, 31549, 2024.

[11] X. Xiao, W. Zhang, Q. Wang *et al.*, "Intelligent recognition method for ferrography wear debris images using improved mask R-CNN methods," *Lubricants*, vol. 13, no. 5, p. 208, 2025.

[12] M. S. Laghari, T. R. Soomro, and G. A. Khuwaja, "The use of fourier descriptors to recognize particle profile," in *Proc. 4th International Conference on Modeling, Simulation, and Applied Optimization*, 2011, pp. 1–6.

[13] M. S. Laghari, "Wear particle profile analysis by using Fourier analysis," in *Proc. 5th IEEE International Workshop on Signal Processing and its Applications*, 2008.

[14] S. N. Kamble and B. Rajiv, "Wear particle quantitative classification from ferrogram micrographic images," *Journal of Failure Analysis and Prevention*, vol. 25, no. 5, pp. 2446–2457, 2025.

[15] M. S. Laghari, F. Ahmed, and J. Aziz, "Wear particle shape and edge detail analysis," in *Proc. 2nd International Conference on Computer and Automation Engineering*, 2010, pp. 122–125.

[16] M. S. Laghari, A. Hassan, and M. Noman, "Wear particle classification using shape features," *Advances in Intelligent Systems and Computing*, vol. 1275, pp. 377–385, 2021.

[17] M. S. Laghari, A. M. S. Alneyadi, A. Y. Alawlaqi, and A. Maraqa, "Identifying wear particles with their shape attribute," in *Proc. 16th International Conference on Computer Graphics, Visualization, Computer Vision and Image Processing*, 2022, pp. 19–22.

[18] B. J. Roylance and T. M. Hunt, *Wear Debris Analysis Handbook*, Oxford, U. K.: Coxmoor Publication, 1999.

[19] H. P. Jost, "Tribology—Origin and future," *Wear*, vol. 136, no. 1, 1990.

[20] S. Raadnui, "Wear particle analysis—utilization of quantitative computer image analysis: A review," *Tribology International*, vol. 38, no. 10, pp. 871–878, 2005.

[21] M. S. Laghari and A. Hassan, "An expert system to identify wear particles," *International Journal of Core Engineering and Management*, vol. 4, no. 12, 2018.

[22] Leica Microsystems. (2025). [Online]. Available: https://www.leica-microsystems.com/

[23] S. E. Umbaugh, *Digital Image Processing and Analysis, Digital Image Enhancement, Restoration and Compression*, 4th ed. USA: CRC Press, 2022.

[24] P.-N. Tan, M. Steinbach, A. Karpatne, and V. Kumar, *Introduction to Data Mining*, 2nd ed. New York, NY, USA: Pearson, 2019.

[25] D. P. Anderson, *Wear Particle Atlas (Revised)*, Tulsa, USA: Noria Corporation, 2012.